EPH - International Journal of Applied Science
ISSN (Online): 2208-2182
Volume 06 Issue 01-March-2020

DOI: https://doi.org/10.53555/eijas.v6i1.105

# TAILORING THE PORE STRUCTURE OF MESOPOROUS SILICA BY USINGAMPHIPHILIC BLOCK COPOLYMER AND CONTROLOF AGING TEMPERATURE

**Wafia M. Emhalha[1*] and Farid M. Hota[2]**
*[*1, 2] Department of Chemistry, Faculty of Science, Sirte University, Sirte, Libya*

***Corresponding author:***
***Email**: wafyamm@gmail.com*

## Abstract:-

*Synthesis of mesoporous silica materials has been studied using Pluronic triblock copolymer F127 nonionic amphiphilic triblock copolymer (EO106 PO70 EO106) as high molecular weight structure-directing agent and TEOS as a silica source. The mesostructure of the silica material obtained, as determined by High Resolution Transmission electron microscopy (HRTEM), Atomic Force Microscopy (AFM), and nitrogen adsorption–desorption isotherm. Changing the amount of surfactant has effect on the porosity of the material, where increasing the amount of surfactant has effect on the hydrophobic surface curvature of the micelle and correspondingly the particle morphology. The particle morphology has changed from hexagonal to cubic Fm3m symmetry, with different pore sizes. Some samples with the same molar ratio have different unit cell size according to the change in aging temperature. HRTEM-ED shows cubic and cage structure of pores under optimum conditions of synthesis. The structural transformation is limited.*

**Keywords: -** *Mesopores, F127, morphology, surface curvature, hexagonal, Fm3m, pore size, aging temperature, and structural transformation.*

## INTRODUCTION

The recent discovery of ordered mesoporous materials has opened prospects for the development of new technologies in catalysis, separation, drug delivery, and nanoscience, owing to their tunable size nanopores, high surface areas, versatile possibilities of surface functionalization, and diversity in composition, structure, and morphology.[1] Of particular interest are mesoporous silicas consisting of interconnected large cage-type pores being organized in a 3D network. For instance, large pore cage-type mesoporous silica designated as SBA-16,[2] synthesized in acidic media EO-PO-EO triblockcopolymer and tetraethylorthosilicate (TEOS) as a silica source, consists EPH - International Journal of Applied Science| ISSN: 2208-2182 of spherical cavities of 9-10 nm in diameter arranged in a body-centered-cubic array (with Im3m symmetry), and connected through a mesoporous opening of 2.0 - 2.5 nm.[3] Such types of high interconnected 3D mesostructure pores materials are expected to be superior to hexagonal structures with 1D channels, especially for applications involving selectivity tuned diffusion, immobilization of large molecules, or host - guest interactions within nanostructured materials. Furthermore, materials such as 2D-hexagonal SBA-15 mesoporous silica[2] are available to used as a model systems for adsorption behavior and diffusion studies in cylindrical pores, while there is still a need for an ideal model systems for closed-packed spherical cavities. Although numerous reports have dealt with the preparation of large pore ordered mesoporous silica,[2-11] the ability to control synthesis conditions providing efficient tuning of the structure and textural properties is still rather limited, with often an uncertain degree of ordering and phase purity. With respect to this, the synthesis of pure phase large pore 3D mesoporous silica, with high quality, still remains challenging. A large cage-type mesoporous silica designated as FDU-1,[6] first reported to have body-centered-cubic Im3m symmetry, was shown by other authors to exhibit face-centered-cubic Fm3m structure with, however, clear evidence of intergrowths with 3D hexagonal phase.[9] Previous efforts by Sakamoto et al.[12] lead to the preparation of a phase-pure silica Fm3m mesoporous structure that was, however, an organofunctionalized silica rather than a pure silica material, and showed relatively small pore diameter (< 4 - 5 nm). Fan et al.[13] used a triblock copolymer and TEOS in the presence of salt (KCl) and an organic additive (trimethylbenzene) as a swelling agent with a high concentration of HCl and extensive reaction time under hydrothrmal conditions (72h). These authors suggested that the cage-like mesoporous siliceous material has cubic symmetry with Fm3m space group. However, they did not demonstrate evidently that it was a cubic close packing of spherical cavities with Fm3m symmetry, as judged by their over simplified structural assignment. Here, we describe a straight forward route of synthesis high ordered mesoporous silica on low HCl concentration regime in aqueous solution allowing facile thermodynamic control of the silica mesophase formation, using different concentrations of F127 and changing the aging temperature during synthesis, through a serious of experiments.

## EXPERIMENTAL

### Synthesis

The large mesophase was prepared in aqueous solution using $EO_{106}PO_{70}EO_{106}$ (Pluronic F127, Sigma) as structural directing agent, and tetraethylorthosilicate (TEOS, Aldrich) as a silica precursor. High quality samples were obtained in the optimum conditions of synthesis. In a typical synthesis, 0.5g of F127 was dissolved in 4 g of acidified distilled water (pH =1.3) and 9g EtOH, then reflux for 2h at 60$^{o}$C. To this mixture, 5g of TEOS was added under stirring. The mixture still stirred at 60$^{o}$C for 24h for the formation of mesostructured material. The solid product was then filtered and dried at 60$^{o}$C without washing. To remove the template, the solid was slurried in an EtOH/HCl mixture, filtered, dried, and calcined in air at 450$^{o}$C with slow heating and cooling rates. In some series of synthesis, the concentration of surfactant increases (1.0 and 2.0g), and aging temperatures 80$^{o}$C. Other sample undergoes template removal by calcination only. The composition of the reaction mixtures and coding of samples prepared are summarized in Table 1.

### Characterization

The Nitrogen adsorption-desorption isotherms were obtained and the samples outgassed at 300$^{o}$C for 4h prior to measurements. High Resolution Transmission Electron Microscopy-Electron Diffraction (HRTEM-ED) Philips using an accelerating voltage of 200 kV and EMS software for electron diffraction analysis and TEM image simulation by using Bloch wave method was used to perform the morphology of the samples. Samples were dispersed in ethanol using ultrasonic method, and the suspension was subsequently dropped onto a cupper microgrid. AFM images were recorded on a Digital Instruments Nanoscope multimode microscope operating in tapping mode.

**Table 1. Synthesis Mixture Weights**

| Sample No. | TEOS in grams | F127 in grams | Water/Acid (pH=1.3) in grams | EtOH in grams | Aging Temprature in °C | Template Removing Method |
|---|---|---|---|---|---|---|
| 1 | 5 | 0.5 | 4 | 9 | 60 | SE+ Calcination |
| 2 | 5 | 1 | 4 | 9 | 60 | SE+ Calcination |
| 3 | 5 | 2 | 4 | 9 | 60 | SE+ Calcination |
| 4 | 5 | 2 | 4 | 9 | 80 | SE+ Calcination |
| 5 | 5 | 2 | 4 | 9 | 80 | Calcination Only |

## RESULTS AND DISCUSSION

### High Resolution Transmission Electron Microscopy-Electron Diffraction (HRTEM-ED)

The structures of samples observed by HRTEM-ED indicate that the pores are hexagonal and cubic according to the synthesis conditions. Figure 1 shows the material obtained from sample 1, has highly ordered 3D hexagonal ($P6_3/mmc$ symmetry) mesostructure, with respectively small pore size. Figures 2 and 3 show the materials obtained from samples 2, and 3, which have a cubic (Fm3m symmetry) mesostructures with larger pore size, where pore size in sample 3 is larger than pore size in sample 2. Figure 4 shows the material obtained from sample 4, which has 2D hexagonal and cubic shape together with relatively small pore size. Figure 5 shows the materials obtained from sample 5, which has narrow pores and impure structure. Figures 1, 2, and 3 indicate the effect of surfactant concentration on the porosity of the material, where increasing the amount of template at the same experimental conditions lead to increasing the pore size, but in Figures 4 and 5 other factors effect on the structure as changing the aging temperature and template removal method, where in Figure 4 which presents sample 4, indicates that increasing the aging temperature causes bimodal structure. That referred to the sensitivity of the triblock copolymers to temperature, where the strength of interactions between the surfactant and silica species affected by temperature and the solubility of F127 at higher temperature may prevent the formation of micelle, or different micellar shape. The critical micellar temperature (CMT) and critical micellar concentration (CMC) must be both taken in account.

The solubility limit of F127 at higher temperature which prevent the formation of micelles because of a too high hydrophobicity, and the micelle temperature (CMT) at lower temperatures, which prevent the formation of micelles because of the high hydrophilicity. That confirms that the assembly mechanism leads to mesostructured materials required a fine balance of interactions, not only between inorganic and organic reagents, but also between the organic templates themselves. At lower concentration of surfactant, the binary (surfactant/water) phase diagram does not exhibit liquid crystal behavior, however, phase separation of the micellar solution induced by the presence of silica species, resulting in microsize domains acted as moulds for the formation of mesoporous silica. At the higher concentration of surfactant, the comparison between mesostructure of the silica and liquid crystal phase behavior of the binary (surfactant/water) system showed a correlation between the order of the meoporous material and the phase behavior of the surfactant (the hydrophilic part is EO, and the hydrophobic one is PO). Sample 4 shows no effect in CMC during aging temperature raising from 60 to 70 ° C. Figure 5 shows sample 5 with template removing using calcination only, where the sample undergoes structure collapse due to sudden template removing before strengthening the silica lattice.

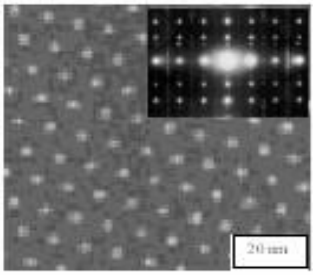


**Figure 1. HRTEM-ED pattern of sample 1, small pore size, low surfactant concentration (3 nm), 3D Hexagonal**

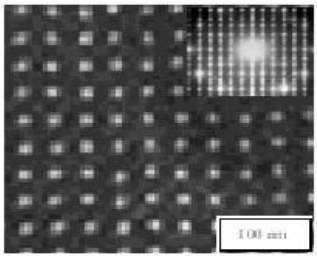

**Figure 2. HRTEM-ED pattern of sample 2, larger pore size, surfactant increases (25 nm), Fm3m**

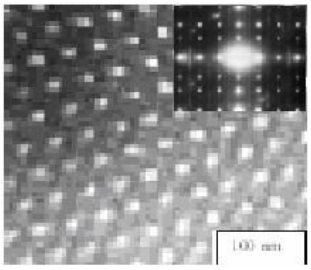

**Figure 3. HRTEM-ED of sample 3, more larger pore size, surfactant more increases (40 nm), Fm3m**

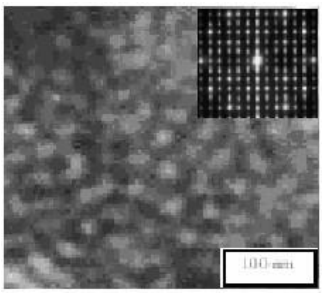

**Figure 4. HRTEM-ED of sample 4 (25 nm), increasing aging temperature (bimodal structure, 2d Hexagonal and Cubic**

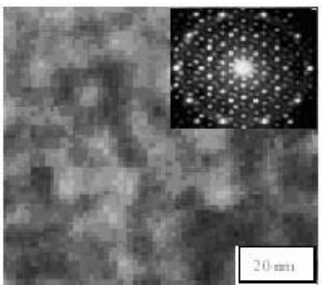

**Figure 5. HRTEM of sample 5 (3 nm), increasing aging temperature and calcination without SE**

**Atomic Force Microscopy (AFM)**

Figures 6, 7, and 8 show the AFM of samples 1, 2, and 3 respectively. Sample 1 of 3D hexagonal shaped ca. 3 nm in diameter were visualized, it being possible to distinguish some vertical channels from others slanted to the surface, suggesting that the channel axes were threedimensionally interconnected, in agreement with TEM results. Samples 2 and 3 show 25 and 40 nm diameter cubic shaped.

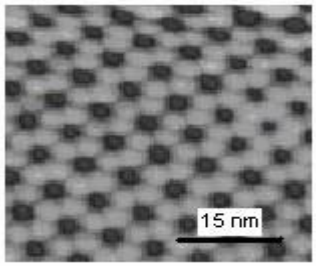


**Figure 6. AFM of Sample 1**

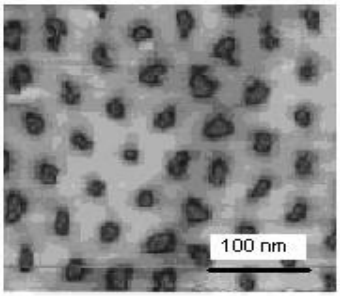


**Figure 7. AFM of Sample 2**

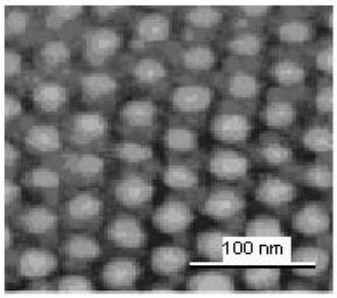


**Figure 8. AFM of Sample 3**

**Nitrogen adsorption-desorption isotherm:**

Figure 9 shows type-IV $N_2$ adsorption-desorption isotherms with different hysteresis obtained from samples 1, 2, 4 and 5. Figure 10 shows pore size distributions of samples 1, 2, and 4, where PSD calculations depend on the change in the amount of gas adsorbed due to capillary condensation. Kilven-cylindrical equation is supposed for calculation. Sample 1 which is 3D hexagonal with small hysteresis. A well-defined step in the adsorption and desorption curve appears between partial pressure $p/p_o$ of 0.3 - 0.5. The pore size distribution curve (PSD) measured from desorption isotherm, shows a mesoporous with a pore diameter 3 nm at the maximum of distribution. The peak width of 0.3nm, measured on the basis of the width at half-maximum for the pore size distribution, indicates that the material has well-defined uniform pore dimensions. *tvalues* calculations of nitrogen adsorbed within the pores considered the curvature of the adsorption layer-gas phase interface. BET surface area and pore volume for the material are 540 $m^2/g$ and 0.7 cc/g, respectively. Sample 2 shows a cubic Fm3m mesoporous structured material. The pore size distribution curve indicates that the material has bottle-shaped pores, with a pore opening size of 25 nm. The analysis results give a BET surface area of 700 $m^2/g$ and a pore volume of 0.85 cc/g. Sample 3 shows also a cubic Fm3m mesoporous structured material. The pore size distribution curve indicates that the material has also bottle-shaped pores, with a pore opening size of 40 nm (not present in the graphs). The analysis results give a BET surface area of 1200 $m^2/g$ and a pore volume of 0.98 cc/g. $C_{BET}$ values during measurements are high, and that indicates the nitrogen technique is very suitable process for porosity measurements, where $C_{BET}$ is related to adsorption heat, the polar $N_2$ molecules expected to be adsorbed strongly by more hydrophilic surfaces, and thus a larger adsorption heat and vice versa. The *t*-plot of all samples, where deviation of the straight line to right insure the presence of microporous silica and insure also the interpretation of the isotherm measured, where the t-plot used according to the similarity of C-values between different materials method, but not the same isotherm of silica material method. Sample 5 shows a cubic Fm3m and 2D-hexagonal mesoporous structured material observed. The pore size distribution curve indicates that the material has spherical pores, with a pore opening size of 25 nm. The analysis results give a BET surface area of 540 $m^2/g$ and a pore volume of 0.77 cc/g.

The decrease in pore size and volume related to presence of bimodal structure of mesoporous silica. Sample 5 shows near type-IV isotherm, where pore size and volume are relatively very low, pore size is 3nm, BET and pore volume values are 210 $m^2/g$ and 0.42 cc/g respectively. The small pore size, pore volume, and surface area are related to the sudden template removal by calcination without using solvent extraction perior to calcination as happened in the rest of the samples, where, F127 undergoes single step oxidation, then combustion reaction, (calcination process) accompanied by a large contraction of the hexagonal unit call, possibly due to further framework condensation. Other possibility reason is that the residual carbonaceous species of burned F127 and water are removed from the structure upon heating from 250 – 550 $^oC$ indicates the probability of pore connectivity present in the structure. Adding to that increasing aging temperature which has a great effect in CMC and CMT of the surfactant behavior and consequently, the final yield morphology. Sample 7 gives nearly the same results as sample 6 in isotherm and pore size distribution calculations. Table 2 summaries the results of nitrogen isotherms.

**Table 2. Nitrogen isotherm Results**

| Sample no. | Average Pore Size (nm) | BET ($m^2/g$) | Average Pore Volume (cc/g) |
|---|---|---|---|
| 1 | 3 | 540 | 0.7 |
| 2 | 25 | 700 | 0.85 |
| 3 | 40 | 1200 | 0.98 |
| 4 | 25 | 540 | 0.77 |
| 5 | 3 | 210 | 0.42 |

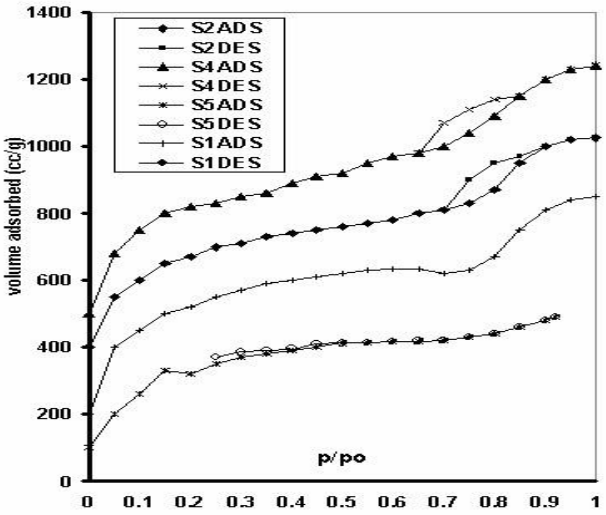


**Figure 9. Nitrogen Adsorption-desorption isotherm of samples 1, 2, 4, and 5**

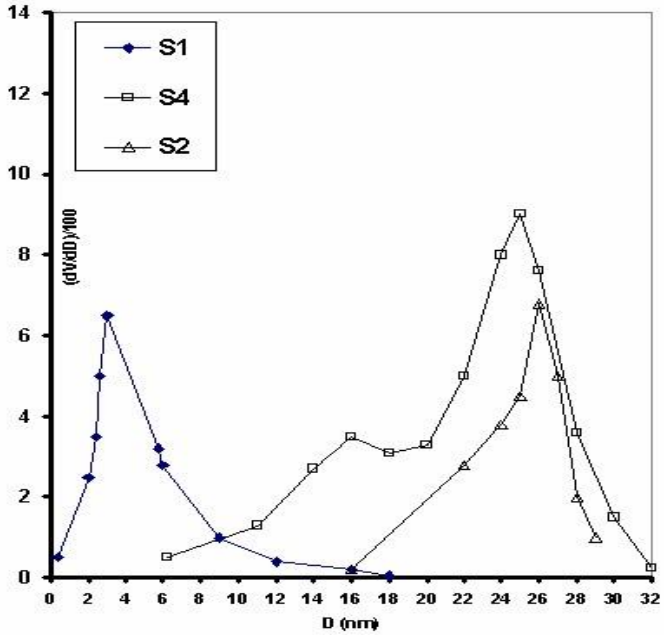


**Figure 10. PSD of samples 1, 2, and 4**

## CONCLUSION

Changing the amount of surfactant has effect on the porosity of the material, where increasing the amount of surfactant has effect on the hydrophobic surface curvature of the micelle and correspondingly the particle morphology. The particle morphology has changed from hexagonal to cubic Fm3m symmetry, with different pore sizes. Some samples with the same structures have different unit cell size according to the change in aging temperature. TEM shows cubic and cage structure of pores under optimum conditions of synthesis. The structural transformation is limited. Template removing method effects on the final yield of mesoporous silica produced where using the solvent extraction technique before calcinations secures the structure from collapse during calcinations process.

**REFERENCES**


[1].Ying, J.Y.; Mehnert, C.P.; Wong, M.S.; Angew. Chem., Int. Ed. 1999, 38, 56.

[2].Zhao, D.; Huo, Q.; Fring, J.; Chemelka, B.F.; Stucky, G.D. J. Am. Chem. Soc. 1998, 120, 6024.

[3].Sakamoto, Y.; Kaneda, M.; Terasak, O.; Zhao, D.; Kim, J.M.; Stucky, G.D.; Shin, H.J.; Ryoo, R. Nature 2000, 408, 449.

[4].Kim, S.-S.; Panty, T.R.; Pinnavaia, T.J. Chem. Commun. 2000, 1661.

[5].Yu, C.; Yu, Y.; Zhao, D. Chem. Commun. 2000, 575.

[6].Kipkemboi, P.; Fogden, A.; Alfredsson, V.; Flodstrom, K. Langmuir 2001, 17, 5398.

[7].Van der Voort, P.; Benjelloum, M.; Vansant, E.F. J. Phys. Chem.2002, 106, 9027.

[8].Flodstrom, K.; Alfredsson, V.; Microporous Mesoporous Mater. 2003, 59, 167.

[9].Matos, J.R.; Kruk, M.; Mercuri, L.P.; Jaroniec, M.; Zhao, L.; Kamiyama, T.; Terasaka, O.; Pinnavaia, T.J.; Liu, Y.J. Am. Chem. Soc. 2003, 125, 821.

[10]. Flodstrom, K.; Alfredsson, V.; Kallrot, N. J. Am. Chem. Soc. 2003, 125, 4402.

[11]. Kleitz, F; Choi, S. H.; Ryoo, R. Chem Commu. 2003, 2136.

[12]. Sakamoto, Y.; Diaz, I.; Terasaki, O.; Zhao, D.; Perez-Pariete, J.; Kim, J. M.; Stucky, J. M.; Stucky, G. D. J. Phys. Chem. B 2002, 106, 3118.

[13]. Fan, J. F.; Yu, C.; Gao, F.; Lei, J.; Tian, B.; Wang, L.; Luo, Q.; Tu, B.; Zhao, W.; Zhao, D. Angew. Chem., Int. Edu. 2003, 42, 314.